UNIVERSITÀ DEGLI STUDI DI TORINO

Department of Molecular Biotechnology and Health Sciences

Ph.D Program in Biomedical Sciences and Oncology

Cycle XXX

Academic Years: 2014-2018

A Peptide-based cAMP Elevator Inhibits Inflammation and Improves CFTR Function in Obstructive Airway disease

Candidate: **Kai Ren**

Tutor: Prof. Emilio Hirsch,

Prof. Alessandra Ghigo

Ph.D Coordinator: Prof. Emilio Hirsch

Index

Abstract

Obstructive airway disease is a common cause of morbidity and a rising of mortality worldwide. It is a progressive respiratory disorder characterized by irreversible chronic inflammation and airflow obstruction. Its rising impact indicates that the ongoing need for novel and effective therapies is still unmet. Conventional treatments include inhaled β_2-adrenergic receptor (β_2-AR) agonists that, by triggering the downstream cyclic AMP (cAMP) signaling in airway structural cells and leukocytes, provide major anti-inflammatory effects. Nevertheless, tachyphylaxis and undesirable side effects severely hamper their clinical use. In the present study, we designed a cell-permeable peptide that targets the protein kinase A (PKA)-anchoring function of phosphoinositide 3-kinase γ (PI3Kγ), and amplifies selected pools of cAMP in the multitude of cell types that contribute to obstructive respiratory diseases. The PI3Kγ mimetic peptide (PI3Kγ MP) promoted smooth muscle relaxation and prevented lung neutrophilia *in vivo* in a model of allergic asthma. In airway epithelial cells, PI3Kγ MP served as a potentiator of cystic fibrosis transmembrane conductance regulator (CFTR), a chloride channel that is defective in chronic obstructive pulmonary disease (COPD) and cystic fibrosis (CF). PI3Kγ MP restored cAMP-mediated trafficking and gating of wild-type and ΔF CFTR (F508del mutant) more efficiently than standard CFTR modulators, in primary human monolayers. Altogether, these results uncover the PI3Kγ MP acts as a novel and safe single drug with pleiotropic effects for the treatment of still incurable lung diseases, such as CF.

Introduction

Obstructive airway diseases (OADs) are a category of respiratory diseases characterized by airway obstruction. Many obstructive pulmonary diseases result from narrowing (obstruction) of the smaller bronchi and larger bronchioles, often because of the excessive contraction of smooth muscle itself. It is generally characterized by inflamed and easily collapsible airways, airflow obstruction, exhalation problems and frequent medical clinic visits and hospitalizations. Nowadays, OADs are a major health burden worldwide. Types of OADs include chronic obstructive pulmonary disease (COPD), asthma, chronic bronchitis, emphysema, cystic fibrosis, and bronchiolitis. COPD is currently the fourth leading death in the world and is predicted to be the 3rd leading cause of the death by 2020 [1]. In 2016, there were 251 million cases of COPD in the world and it was estimated that COPD causes 3.15 million deaths per year [2]. Despite the diversity in terms of disease onset, the frequency of symptoms and reversibility of airway obstruction, these conditions share common pathophysiological features, primarily airway inflammation, airway hyperreactivity (AHR) and mucosal edema, that eventually result in bronchoconstriction [3].

Conventional medications include inhaled corticosteroids (ICS) and β_2-adrenergic receptor (β_2-AR) agonists, that reduce airway inflammation and reverse airway constriction, respectively. Infiltration of neutrophils and macrophages to the site of inflammation is the central event of COPD pathophysiology, although CD8+ T lymphocytes and dendritic cells are also implicated [4]. ICS is considered as the gold standard anti-inflammatory drugs for the treatment of respiratory diseases, because of their broad range of anti-inflammatory actions. However, this class of drugs is associated with significant side-effects when they enter the systemic circulation, as well as having local side-effects when applied topically [5]. In clinical medical, ICS is rarely

used alone, rather they are employed in association with agonists of β_2-AR to obtain a better control of the disease. β_2-AR agonists' prominent action is the relaxation of airway smooth muscle and they may also favor the resolution of inflammation and mucociliary clearance by triggering β_2-ARs, and the downstream cyclic AMP (cAMP) signaling, in circulating leukocytes and airway epithelial cells. Nevertheless, the efficacy of β_2-AR agonists is still unsatisfactory, primarily because of tachyphylaxis, and safety concerns have led to more stringent guidelines for their clinical use [6]. Similarly, inhibition of cAMP breakdown by drugs targeting phosphodiesterase 4 (PDE4), the major cAMP-hydrolyzing enzyme in the airways, has been clinically tested but exhibits unwanted side effects, such as emesis, nausea, diarrhea, and weight loss, likely stemming from systemic PDE4 blockade [7]. Cystic fibrosis transmembrane conductance receptor (CFTR) is a cAMP-activated chloride channel expressed in epithelial cells apical membrane and controls airway surface liquid homeostasis, mucociliary clearance and avoiding mucus accumulation [8]. Acquired dysfunction of cystic fibrosis transmembrane receptor (CFTR), as well as a genetic disorder of CFTR in cystic fibrosis (CF) patients, leads to more cough and sputum production in most COPD patients who complain about the mucus hypersecretion, accumulation, and poor clearance [9]. In addition, pulmonary disease is the main reason for mortality in CF patients with mutant CFTR. Although many compounds, including corrector (e.g. VX-809) and potentiator (e.g. VX-770), aim to rescue and potentiate the mutant CFTRs function, they improve respiratory function little to CF patients with homozygous for the F508del CFTR mutation (deletion of phenylalanine at position 508), which occurs in more than 70% CF patients [10]. Thus, novel and safe strategies of manipulating β_2-AR/cAMP signaling axis in the multitude of cell types that contribute to respiratory diseases are urgently needed.

Previous work from our group identified the phosphoinositide 3-kinase γ (PI3Kγ) as a key regulator of cAMP compartmentalization within β_2-AR/PDE4 microdomains in heart. Indeed, PI3Kγ serves as an A-kinase anchoring protein (AKAP) and PI3Kγ-bound protein kinase A (PKA) activates PDE4, eventually restricting β_2-AR/cAMP responses to discrete subcellular compartments [11], [12]. Accordingly, disruption of PI3Kγ scaffold, but not kinase, activity results in localized β_2-AR/cAMP signaling amplification in isolated cardiomyocytes [12]. Thus, targeting the scaffold function of PI3Kγ may represent a novel way to achieve compartmentalized cAMP elevation in the airways.

Moreover, the mechanism that promotes surface secretion of F508del CFTR has not been fully revealed. Beginning from the discovery that the restoration of F508del CFTR on the surface membrane in low-temperature (27 °C) has been reported by Denning *et al.* [13], scientists are always pursuing the efficient modulators of F508del CFTR surface secretion in the past decades. Recently, *Lobo et al.* reports that activation of the cAMP sensor EPAC1 leads to stabilization of CFTR at the plasma membrane, through a mechanism that involves the PDZ adaptor NHERF1 [14]. This finding suggests that cAMP also stimulates the surface secretion of CFTR in a definite way besides the activation of CFTR. CFTR is a glycoprotein that undergoes complex glycosylation as it passes through the Golgi-mediated conventional exocytosis [15], [16]. Therefore, the fully glycosylated mature CFTR, also known as band C in Western blot, is expressed at the apical membrane of epithelial tissues [17]. The most common mutation of CFTR, F508del CFTR, results in protein misfolding, retention in ER, and finally degradation by the ER-associated degradation (ERAD) pathway [16]. As a result, negligible amounts of F508del CFTR reach the plasma membrane, and F508del CFTR remains in the ER core-glycosylated immature form, also known as band B, in cells

[17]. Interestingly, Gee *et al.* reports that overexpression and phosphorylation of the Golgi reassembly stacking protein (GRASP) induces an unconventional secretion of both wild-type and F508del CFTR, through the endoplasmic reticulum (ER) directly to the plasma membrane and bypassing the Golgi, and rescues the defects caused by F508del CFTR in murine cystic fibrosis model [18]. This finding opens a new view that targeting CFTR unconventional secretion to increase the rescue of mutant CFTR represents a fresh therapeutic strategy of CF. Thus, we expect that the surface secretion of CFTR is able to be enhanced by high compartmental cAMP, which is elicited by inhibition of the scaffold function of PI3Kγ. Yet, pharmacological strategies for targeting the PKA-anchoring function of PI3Kγ are still undefined.

Here we report that disruption of PI3Kγ scaffold activity by a cell-permeable mimetic peptide (MP) interrupting PI3Kγ/PKA interaction increases cAMP levels *in vivo* in the airways. In addition, the PI3Kγ MP limits lung neutrophilia and mucus hypersecretion in a mouse model of inflammatory airway disease. Moreover, disruption of PI3Kγ-bound PKA promotes cAMP-mediated chloride efflux through the CFTR in primary normal and CF bronchial epithelial cells. Furthermore, the PI3Kγ MP increases the surface stability of wild-type CFTR and F508del CFTR rescued by corrector VX-809, and the PI3Kγ MP *per se* promotes the F508del CFTR surface secretion by an unconventional pathway. More importantly, the PI3Kγ MP can be safely administered to mice from trachea, without generating an immunogenic response and organs damage, and it is stable in the airways.

Altogether, these data identify the PI3Kγ MP as a new and effective anti-inflammatory drug and CFTR corrector and potentiator for the treatment of chronic obstructive lung diseases.

Results

A PI3Kγ mimetic peptide enhances airway β_2-AR/cAMP signaling through disruption the PKA-anchoring function of PI3Kγ

In order to disrupt the PKA-anchoring function of PI3Kγ *in vivo*, a peptide containing the PKA-binding motif of PI3Kγ [11] was fused to the cell-penetrating sequence Penetratin-1 (P1) [19] (Fig. 1a). A FITC-labeled version of the PI3Kγ mimetic peptide (PI3Kγ MP) was used to assess its capability to penetrate *in vitro* in cells. As soon as 1 hour after incubation, the FITC-labeled PI3Kγ MP accumulated in human bronchial smooth muscle cells (hBSMCs) (Fig. 1a). PI3Kγ MP was also tested to disrupt the interaction between the catalytic subunit of PI3Kγ, p110γ, and the regulatory subunit of PKA, RII, in HEK 293 cells. The complex of PI3Kγ/PKA-RII was decreased in a dose-dependent manner in HEK 293 cells after treatment with different dose of PI3Kγ MP for 2 hours (Fig. 1b).

To determine the transduction efficiency of the PI3Kγ MP *in vivo* in the airways, a FITC-labeled form was instilled intratracheally in mice. FITC fluorescence was detected in trachea and lungs as soon as 30 min after administration (Fig. 1c) when cAMP levels were already 30% higher than in tissues from animals receiving either saline or the control peptide (CP) (Fig. 1d). The peptide stably existed in the airways, lung and trachea, at least 1 day after a single intratracheal instillation (Fig. 1e). A significant increase of cAMP levels was detected at 1 day after PI3Kγ MP injection when the maximal accumulation of PI3Kγ MP was presented (Fig. 1f). Notably, the PI3Kγ MP neither reached other organs nor modified cAMP homeostasis outside of the respiratory system, such as in the myocardium (Fig. 1e, f). These data indicate that a PI3Kγ MP increases cAMP level with high-efficiency and tissue-specific features.

A PI3Kγ mimetic peptide limits neutrophilic airway inflammation in asthmatic animals

According to the cAMP-elevating agents may have major anti-inflammatory effects [20], we thus reasoned that the PI3Kγ MP could be therapeutically exploited to limit asthma-associated lung inflammation. Repeated treatment with the PI3Kγ MP significantly prevented the infiltration of inflammatory cells into the peribronchial tissue and few goblet cells were detected around the bronchial airways in OVA-induced asthma model mice (Fig. 2a, b). Furthermore, a significantly lower number of neutrophils was detected in the bronchoalveolar lavage (BAL) fluid of mice treated with the PI3Kγ MP than in control animals (Fig. 2c). Three weeks after daily intratracheal injection with PI3Kγ MP, mice organs and body weight were not affected (Fig. 2d, e and Tables I-II). Especially, the specific IgG against PI3Kγ MP was also not detected in the mice serum by tracheal administration (Fig. 2f). These results suggest that the PI3Kγ MP has non-immunogenicity and low cytotoxicity and could be safely employed for treating chronic respiratory diseases.

Taken together, these findings highlight the ability of the PI3Kγ MP to limit neutrophilic airway inflammation through potentiation of leukocyte cAMP/PKA signaling.

A PI3Kγ mimetic peptide promotes wild-type CFTR membrane stability and chloride channel function

In addition to their anti-inflammatory properties, cAMP-elevating drugs may have other effects linked to modulation of β_2-AR signaling in airway epithelial cells, where high cAMP levels are essential to maintain adequate CFTR-mediated chloride efflux and, in turn, mucus hydration [21]. Thus, the possibility of using a PI3Kγ MP to

modulate therapeutically airway epithelial β_2-AR/cAMP signaling was next examined. PI3Kγ was expressed in human airway epithelial cells (16HBE14o-) and immunofluorescence studies revealed an enrichment of PI3Kγ at the apical membrane of these cells (Fig. 3a), suggesting that PI3Kγ was sequestered into the vicinity of CFTR. Accordingly, PI3Kγ physically associated with wild-type CFTR and also with F508del CFTR (Fig. 3b), a mutant form carried by the majority of patients affected by cystic fibrosis. We then investigated whether disruption of PI3Kγ scaffold function may affect cAMP signaling in the vicinity of CFTR and may impact on cAMP-dependent gating of the channel. cAMP-mediated phosphorylation of CFTR was 5-fold higher in 16HBE14o- cells treated with the PI3Kγ MP than in cells exposed to the control peptides (Fig. 3c). Notably, disruption of PI3Kγ scaffold activity enhanced channel phosphorylation at the same extent as the PDE4 inhibitor Rolipram, while PKA inhibition completely abolished the effect of the PI3Kγ MP (Fig. 3c, d). These findings conclusively proved a key role for PI3Kγ-mediated, PKA-dependent activation of PDE4 in cAMP-mediated regulation of CFTR. Given that PKA-mediated phosphorylation of CFTR is a primary mechanism of channel gating [22], the ability of the PI3Kγ MP to enhance Cl^- conductance was subsequently investigated in primary human bronchial epithelial (pHBE) cells. CFTR-dependent currents (I_{SC}) were significantly enhanced by increasing concentrations of the PI3Kγ MP, while unaffected by the control peptide (Fig. 3e). In the meanwhile, the finding that the increase of surface wild-type CFTR stimulated by PI3Kγ MP further demonstrated that the enhanced chloride conductance function of wild-type CFTR partially results from the improvement of wild-type CFTR stabilization on the plasma membrane by PI3Kγ MP (Fig. 3f). In agreement with the previous report [23], PI3Kγ MP was clearly detected to increase the co-localization of wild-type CFTR and actin on the plasma membrane by

immunofluorescence assay (Fig. 3g). Altogether, these data unveil a role for the PI3Kγ MP as a novel CFTR potentiator.

A PI3Kγ mimetic peptide stabilizes and opens the surface F508del CFTR rescued by corrector VX-809

New effective CFTR potentiator is highly desirable in CF therapy, especially for patients carrying the most prevalent F508del mutation which leads to a misfolded and prematurely degraded channel. A combination therapy including a corrector (VX-809) and a potentiator (VX-770), to rescue expression and function respectively, of CFTR has been recently approved for these patients, but the efficacy is unsatisfactory because chronic VX-770 interferes with VX-809-mediated correction [24], [25]. Unlike VX-770, chronic treatment with the PI3Kγ MP did not affect VX-809-mediated correction and led to a significantly higher amount of complex-glycosylated CFTR (C band) than in VX-770-treated cells (Fig. 4a). Moreover, following inhibition of the new CFTR synthesis by Cycloheximide (CHX), a eukaryote protein synthesis inhibitor, the PI3Kγ MP treatment significantly stabilizes the corrected complex-glycosylated CFTR (C band), compared to VX-770 (Fig. 4b).

Furthermore, the PI3Kγ MP significantly increased I_{SC} currents on top of forskolin-induced potentiation and at the same extent as acute VX-770 in pharmacologically corrected F508del CFTR primary human airway epithelial (F508del-pCFBE) cells (Fig. 4c). Sequential application of VX-770 and the PI3Kγ MP resulted in a further significant increment of CFTR conductance (Fig. 4c), suggesting a synergic action between the peptide and the gold standard potentiator. Intriguingly, the PI3Kγ MP synergized with VX-770 and increased I_{SC} currents by 5-fold even in absence of forskolin-mediated pre-potentiation, while the control peptide did not affect

CFTR activity (Fig. 4d). These data unravel a novel role for the PI3Kγ MP as a CFTR potentiator that promotes cAMP-dependent gating of both wild-type and F508del CFTR, without interfering with CFTR stability.

A PI3Kγ mimetic peptide promotes F508del CFTR unconventional secretion.

Cl^- secretion through CFTR depends not only on the activity of each individual channel but also on the channel density at the cell surface [26]. Notably, the most common mutant in CF, F508del CFTR, exhibits decreased stability at the plasma membrane even after pharmacological correction [27]. Since an increase in cAMP levels increases CFTR localization at the plasma membrane by blocking its endocytosis [14], we investigated whether the PI3Kγ MP could similarly enhance plasma membrane CFTR expression. The ectopic expressed F508del CFTR at the plasma membrane were significantly increased upon PI3Kγ MP treatment compared to the control peptide in HEK 293 cells in absence of correctors (Fig. 5a). Furthermore, this augment was already detectable 5 minutes after the treatment with the peptide and reached the peak at 30 minutes in F508del CFTR overexpressed CFBE cells (Fig. 5b), suggesting that the PI3Kγ MP can improve the surface trafficking of CFTRs through a special pathway that works as short as 5 minutes.

Recently, researchers observe that CFTR can be transported directly from the ER to the plasma membrane but bypass the Golgi, named an unconventional secretion pathway [28]. To further determine whether the PI3Kγ MP mediates CFTR trafficking via an unconventional secretion pathway, we blocked the conventional Golgi-mediated exocytic pathway in HEK293 cells expressing wild-type or F508del CFTR (Fig. 5c-e). Inhibition of the anterograde coat protein complex II (COPII)-mediated ER-to-Golgi trafficking was achieved by syntaxin 5 (STX5) overexpression (Fig. 5c), which is in

line with the previous study [18]. STX5 is a target soluble N-ethylmaleimide (NEM)-sensitive factor attachment protein receptor (t-SNARE), which is specifically required for the fusion of COPII transport vesicles with acceptor Golgi membranes [29]. Overexpression of STX5 inhibits ER-to-Golgi traffic by disrupting the stoichiometric balance of functional SNARE complexes [30], [31]. As shown in Figure 5c, overexpression of STX5 but not WT-Sar1 and a dominant-negative form of Sar1 (Sar1-T39N), that is a critical component of the COPII complex, completely blocked maturation of wild-type CFTR complex-glycosylation (C band), however, the core-glycosylated wild-type CFTR was still targeted to the cell surface (B band). So, we chose the overexpression of STX5 as the positive control to induce CFTR unconventional secretion in the following experiments. Of note, PI3Kγ MP, as well as STX5, significantly promoted F508del CFTR secretion to the cell surface (Fig. 5d). Furthermore, PI3Kγ MP synergized with STX5 to further enhance F508del CFTR surface exocytosis (see lane 5^{th} in Fig. 5d). Finally, PI3Kγ MP-mediated surface-expressed F508del CFTR was endoglycosidase H-sensitive (Fig. 5e), the endoglycosidase H only deglycosylates ER core-glycosylation but not complex-glycosylation, which corroborated the notion that PI3Kγ MP-mediated surface expressed F508del CFTR were only ER core-glycosylated and a Golgi-independent route mediates their surface trafficking.

Altogether, these findings indicate that PI3Kγ MP promotes the surface trafficking of F508del CFTR via an unconventional secretion pathway.

Discussion

Our results suggest that targeting the PKA-anchoring function of PI3Kγ with a PI3Kγ mimetic peptide increases the selected pools of cAMP in different cell types of the airways, and can be used as a novel and safe strategy for the treatment of obstructive airway diseases.

Previous studies from our group unveiled a role of PI3Kγ which is independent of its kinase activity: in the heart, PI3Kγ can serve as a scaffold protein, an AKAP, regulating cAMP compartmentalization within β_2-AR/PDE4 microdomains [11]. Here, we extend this view and demonstrate that a similar PI3Kγ activity is present in the airways and that targeting this function may represent a novel way to achieve compartmentalized cAMP elevation in the lung. In the airways, the cAMP pathway is responsible for major bronchorelaxant and anti-inflammatory signals and is therefore the target of frontline therapy for asthma and COPD. Unfortunately, these gold standard treatments for obstructive airway diseases exhibit poor efficacy and tolerability in patients, with prominent side effects due to the systemic activities of these drugs. Therefore, targeting the scaffold activity of PI3Kγ may constitute a novel therapeutic approach to target OADs.

Although many small molecules targeting the kinase activity of PI3Kγ have been developed and are currently in clinical trials for cancer treatment, no means have been conceived so far to selectively interfere with the scaffold function of the enzyme. It has been previously reported that a peptide encompassing the PKA binding site of PI3Kγ, PI3Kγ 126-150, disrupts PKA anchoring in *in vitro* interaction studies and lowers the activity of PI3Kγ-bound PDE3B [11]. The present study further extends this notion by demonstrating that a PI3Kγ 126-150 mimetic peptide entered airway smooth muscle cells and potentiated β_2-AR/cAMP signaling *in vivo* when linked to the well-known

cell-penetrating module from *Antennapedia*, Penetratin 1 [19]. The finding that the PI3Kγ MP enhanced cAMP and attenuated airway inflammation in a preclinical model of allergic asthma demonstrates that the inhibitor is efficiently delivered to the lower airways when administered locally and demonstrates the feasibility of using a PI3Kγ inhibitory peptide in aerosol therapy for bronchoconstrictive diseases. Despite the reported clinical benefits of β-AR agonists, chronic or repeated exposure to these drugs leads to the loss of their pro-relaxant effects in a significant subpopulation of asthmatic, likely resulting from agonist-dependent desensitization of β_2-ARs [32]. The present study provides a solution to this issue and proposes the use of an inhibitor that affects the activity of the enzyme PI3Kγ and, as such, does not act directly on the stimulation of β_2-AR, but enhances the downstream signaling cascade of events. In this way, a peptide inhibitor of PI3Kγ offers the unique opportunity to modulate the β_2-AR-dependent cAMP domains, ensuing bronchodilation similar to β_2-AR agonists, but avoiding receptor desensitization.

In addition, our work demonstrates that the PI3Kγ MP has a strong anti-inflammatory activity *in vivo* in a preclinical model of allergic asthma. The PI3Kγ MP is able to significantly decrease the number of infiltrated neutrophils in these mice lungs, suggesting that this peptide may be effective and suitable to treat severe forms of asthma, such as the neutrophilic subgroup, and COPD that are resistant to current therapies. The finding that an aerosolized formulation of the PI3Kγ MP is efficiently and selectively delivered to the lower airways demonstrates the feasibility of a localized therapy with the PI3Kγ disruptor. This may eventually provide a wider effect to side-effect profile than freely diffusible small molecule inhibitors. Accordingly, a FITC-labeled version of the PI3Kγ MP accumulates in the trachea and lungs, while not

reaching the myocardium and the central nervous system, when delivered intratracheally.

An inhalation therapy based on a PI3Kγ disruptor may be thus envisaged for treatment of different respiratory diseases wherein cAMP-elevating agents are highly desirable, ranging from allergic asthma to cystic fibrosis. The finding that the PI3Kγ disruptor augments cAMP not only in smooth muscle but also in the epithelial compartment of the airways opens the possibility to exploit this compound to potentiate the defective cAMP-mediated gating of the mutant CFTR. Accordingly, PI3Kγ inhibition dramatically enhanced the activity of a clinically advanced CFTR potentiator, VX-770 which has been shown to be almost ineffective in rescuing the function of the most common mutant CFTR in CF patients. To our knowledge, this is the first evidence of a compound able to improve the potentiating effect of VX-770. Our results also unveiled the capability of a PI3Kγ MP to stabilize the CFTR on the plasma membrane both wild-type and F508del CFTR. The CHX experiment results strongly suggest that the PI3Kγ MP stabilizes the rescued F508del CFTR through either inhibiting CFTR endocytosis or increasing CFTR channel recycle. Although the previous study determines that F508del CFTR plasma membrane secretion should be under two conditions including GRASP overexpression and ER stress that is induced by the inhibition of COPII formation and fusion process between COPII vesicles and acceptor Golgi membranes [18], our data demonstrate that the PI3Kγ MP *per se* promotes F508del CFTR surface exocytosis in CFBE cells without GRASP overexpression and ER stress. In addition, the PI3Kγ MP dramatically synergizes F508del CFTR surface expression with the ER stress that is elicited by STX5 overexpression. Meanwhile, the finding that the rescued surface F508del CFTR by PI3Kγ MP is endoglycosidase H-sensitive demonstrates that PI3Kγ MP promotes unconventional secretion of immature

core-glycosylated CFTR whereby directly from ER to the plasma membrane bypassing the Golgi.

Overall, the current work highlights the therapeutic potential of a cell-permeable peptide targeting the scaffold function of PI3Kγ. The therapeutic properties may be relevant for the treatment of airway diseases including allergic asthma where cAMP-elevating agents with bronchorelaxant properties are highly desirable. In addition, this compound finds application in CF patients where cAMP-elevating drugs are suitable tools to stimulate cAMP-mediated gating of the defective channel. Furthermore, peptide-based inhibition of PI3Kγ may be applicable to all pathological conditions characterized by CFTR hypofunction, including COPD where exposure to cigarette smoke has been shown to impair CFTR activity and directly linked to mucus stasis and COPD pathogenesis. Finally, by increasing cAMP, the PI3Kγ MP may exert important anti-inflammatory actions as previously described for the PDE4 inhibitor, Roflumilast. Although the anti-inflammatory properties of the peptide have not been deeply investigated so far, it is plausible to envisage a scenario wherein inhibition of PI3Kγ scaffold activity may provide multiple independent therapeutic benefits in respiratory disease treatments by acting as a bronchodilator, CFTR corrector and potentiator, and anti-inflammatory agent.

From the first peptide therapeutic (insulin) approved in the 1920s, over 60 peptide drugs are applied in medical practice worldwide, and peptides continue to enter clinical development at a steady pace. Until now, over 150 peptide drugs that entered the human clinical study. However, peptide therapeutics also show some intrinsic weakness, including chemical and physical stability, and immunogenicity and drug resistance [34], [35]. Our results demonstrate that PI3Kγ mimetic peptide efficiently reaches the terminal bronchiole and concentrates in airway at least for 1 day by the tracheal

administration in mice. Furthermore, this peptide does not induce specific IgG in mice serum, thus it most likely avoids tachyphylaxis *in vivo*. In conclusion, our findings indicate that PI3Kγ MP should be further studied in pre-clinical and clinical trials as a potential therapeutic medication for obstructive airway diseases.

Materials and Methods

Antibodies, plasmids and reagents

CFTR antibodies (A2-570, A3-217 and A4-596) were kindly provided by Dr. J. R. Riordan (University of North Carolina at Chapel Hill, Chapel Hill, NC, USA) via the CFTR Antibody Distribution Program of the Cystic Fibrosis Foundation. The phospho-Ser/Thr-PKA substrate antibody was purchased from Cell Signaling Technology (Danvers, MA, USA) and the CFTR antibody M3A7 from Millipore (Billerica, MA, USA). Monoclonal antibodies against p110γ, p101 and p87 were used as previously described [11]. Antibodies against the regulatory and catalytic subunits of PKA were from Santa Cruz Biotechnology (Santa Cruz Biotechnology, Santa Cruz, CA).

GFP-CFTR and GFP-F508del-CFTR expression vectors were kind gifts from Dr. Peter Haggie (University of California San Francisco). The plasmids encoding Myc-Sar1-WT, Myc-Sar1-T39N, HA-STX5 and GRASP55 were kindly provided by Prof. Tang Bor Luen (National University of Singapore).

cycloheximide (CHX) was from Sigma (Sigma-Aldrich, Saint Louis, MO). H89 dihydrochloride was from (Biotechne, Minneapolis, MN). Roflumilast was provided by Chiesi Farmaceutici. VX-809 (Lumacaftor) and VX-770 (Ivacaftor) was provided by Vertex Pharmaceuticals Incorporated.

Penetratin-1 (P1) and the PI3Kγ MP were synthesized by GenScript (GenScript, Piscataway, NJ, USA) and Chinapeptides (Chinapeptides Co. Ltd, Shanghai, China), and the amino acid sequence of them are as follows, Penetratin-1: RQIKIWFQNRRMKWKK; PI3Kγ MP: RQIKIWFQNRRMKWKKGKATHRSPGQI HLVQRHPPSEESQAF.

Cell culture and transfection

Normal human bronchial smooth muscle cells (hBSMCs) were purchased from Lonza (CC-2576, Lonza Walkersville, Inc. USA), cultured in Dulbecco's modified Eagle's medium (DMEM, Gibco, Carlsbad, CA), supplemented with 10% Fetal Bovine Serum (FBS) and 1% penicillin-streptomycin (10,000U/mL, Gibco, Carlsbad, CA). Cells were used for experiments up to passage 15. The efficiency of PI3Kγ knock-down was assayed by Western blotting using a selective PI3Kγ antibody at 24, 48 and 72 hours after transfection. Imaging experiments were performed at 48 hours after nucleofection in GFP-positive cells. Normal human bronchial epithelial (16HBE14o-) and cystic fibrosis human bronchial epithelial (CFBE41o-) cell lines were kindly provided by Dr. Dieter Gruenert (University of California San Francisco, San Francisco, CA, USA). Cells were cultured in Minimum Essential Medium (MEM) supplemented with 10% fetal bovine serum (FBS), 100 U/mL, penicillin and 100 μg/mL, streptomycin (Thermo Fisher Scientific, Waltham, MA USA) on culture dishes pre-coated with human fibronectin (1 mg/ mL,; Sigma-Aldrich, Saint Louis, MO), bovine collagen I (3 mg/mL,; Sigma-Aldrich, Saint Louis, MO) and bovine serum albumin (0.1%; Sigma-Aldrich, Saint Louis, MO). HEK293 cells were cultured in DMEM supplemented with 10% FBS and 100 U/mL penicillin and 100 μg/mL streptomycin (Thermo Fisher Scientific, Waltham, MA USA). Cells were transfected with the indicated plasmids (up to 10 μg of total cDNA) with calcium phosphate. 24 hours after transfection cells were lysed or treated as described below. All cells were cultured at 37 °C and under a 5% CO_2 atmosphere.

Protein extraction and immunoprecipitation

Liquid nitrogen-frozen tracheas were homogenized in 120 mmol/L NaCl, 50 mmol/L Tris-HCl (pH 8.0), 1% Triton X-100, protease inhibitor Complete (Roche

Applied Science, Indianapolis, IN) and phosphatase inhibitors (50 mmol/L sodium fluoride, 1 mmol/L sodium orthovanadate, and 10 mmol/L sodium pyrophosphate). After 30 min incubation on ice, lysates were centrifuged at 13000 rpm for 10 min at 4 °C and either used for Western blotting or subjected to immunoprecipitation/PDE activity measurements.

hBSMCs, 16HBE14o-, CFBE41o- and HEK 293 cells were scraped in 120 mmol/L NaCl, 50 mmol/L Tris-HCl (pH 8.0) and 1% Triton X-100, supplemented with protease and phosphatase inhibitors, as described above. Detergent-insoluble material was precipitated by centrifugation at 13000 rpm for 10 min at 4 °C. Supernatants were subjected to immunoprecipitation or used directly for Western blotting. For immunoprecipitation assays, pre-cleared extracts were incubated with 20 µl of a 1:1 slurry of protein A- or G-Sepharose (Amersham Biosciences, Buckinghamshire, UK) and 1 µg of antibody/mg of protein for 2 h at 4 °C. Immunocomplexes were then extensively washed with lysis buffer and either used for Western blotting or subjected to PDE activity assay.

Cell surface biotinylation assay

Cells were washed twice with ice-cold PBS and incubated with 0.5 mg/mL Sulfo-NHS-SS-biotin (Thermo Fischer Scientific. Inc) in PBS for 1 h at 4 °C under gentle agitation. Cells were washed once with 25 mM Tris (pH=8.0) to quench non-reacted biotinylation reagent and twice with ice-cold PBS to remove non-reacted biotinylation reagent. Protein extraction was performed as described above. An aliquot of supernatants corresponding to 600 µg of proteins was incubated with high capacity streptavidin agarose resin (Thermo Fischer Scientific. Inc), for 2 h at 4 °C with gentle mixing, following the manufacturer's recommendation. Streptavidin-bound complexes were pelleted at 1000 g and washed four times with lysis buffer. Biotinylated proteins

were eluted from the resin with SDS-PAGE Sample Buffer 2X and directly used for Western blotting.

For digestion of glycosylated CFTR by Endoglycosidase H (Endo H; New England Biolabs), protein samples were first denatured by adding glycoprotein denaturing buffer and incubated at 37 °C for 10 min. Protein samples were then treated with Endo H (1000 U/reaction) and further incubated at 37 °C for 1 h before subjected to Western blot analysis.

Western blotting

Proteins concentration from tissue or cells extract was determined using the Bio-Rad protein assay system (Bio-Rad, Munchen, Germany). Proteins were analyzed in 7.5% or 4-20% gradient SDS-PAGE gels, as appropriated, and transferred to PVDF membranes. Membranes were blocked with 5% BSA in TBST at room temperature for 1 h. Subsequently, membranes were incubated at 4 °C overnight with primary antibodies diluted into the TBST at the indicated dilution ratio. Primary antibody binding was detected using a horseradish peroxidase-conjugated secondary antibody and developed using a chemiluminescence ECL assay kit (Millipore Corporation, Billerica, Massachusetts). Quantification of protein bands was performed with Quantity One analysis software (Bio-Rad).

Peptide competition assay

HEK293T cells were transfected with pcDNA3.1-PI3Kγ using the calcium phosphate method and 48 hours post-transfection cells were treated with different doses of the PI3Kγ MP or the P1 control peptide for 2 hours. Cells were lysed in cold lysis buffer as described above and the regulatory subunit of PKA (PKA RII) was immunoprecipitated with the appropriate antibody and the presence of the PI3Kγ

catalytic subunit (p110γ) was evaluated through SDS-PAGE and immunoblotting analysis.

Short-circuit current (Isc) measurements

To measure chloride currents in normal and F508del primary human bronchial epithelial cells, cells were cultured on 1.12 cm^2 Snapwell inserts. Filters were mounted in Ussing chambers, and a chloride gradient was applied by incubating the cells in a basolateral high-chloride buffer containing (in mmol/L): 140 NaCl, 5 KCl, 0.36 K_2HPO_4, 0.44 KH_2PO_4, 1.3 $CaCl_2$, 0.5 $MgCl_2$, 4.2 $NaHCO_3$, 10 HEPES, and 10 glucose, at pH 7.4 and an apical low-chloride buffer containing (in mmol/L): 133.3 Na-gluconate, 5 K-gluconate, 2.5 NaCl, 0.36 K_2HPO_4, 0.44 KH_2PO_4, 5.7 $CaCl_2$, 0.5 $MgCl_2$, 4.2 $NaHCO_3$, 10 HEPES, and 10 mannitol, at pH 7.4. Buffers were aerated with a mixture of 95% O_2 and 5% CO_2 and the temperature was maintained at 37 °C during the experiment. Cultures were maintained at a voltage of 0 mV using an EVC4000 MultiChannel V/I Clamp (World Precision Instruments, Sarasota, FL, USA). After a stabilization period of 30 minutes, drugs were added at specific times, while the current was continuously recorded.

cAMP extraction and quantification

Lungs, tracheas and heart were collected from euthanized mice, powdered in liquid nitrogen and extracted with cold 6% trichloroacetic acid. Samples were sonicated for 10 seconds and centrifuged at 2000 xg at 4 °C for 15 minutes. Supernatants were washed four times with five volumes of water saturated diethyl ether and lyophilized. cAMP content was detected with Amersham cAMP Biotrak Enzymeimmunoassay System (GE Healthcare Life Sciences, Pittsburgh, USA), according to the manufacturer's protocol.

Isolation of mouse tracheal smooth muscle cells

Tracheal smooth muscle cells were cultured from explants of excised tracheas using modifications of previously described methods [36]. The whole trachea between the larynx and the main stem bronchi was removed and placed in a sterile Petri dish containing room temperature Hanks' balanced saline solution, supplemented with a 2x concentration of antibiotic-antimycotic (Gibco, Carlsbad, CA). With the aid of a dissecting microscope, additional surrounding tissue was removed, the tracheal segment was split longitudinally and dissected into 2-3 mm squares. All the segments from a single trachea were then placed intima side down in a sterile 60-mm dish. After allowing the explants to adhere, 2.5 mL of Dulbecco's modified Eagle's medium (DMEM, Gibco, Carlsbad, CA), supplemented with 20% Fetal Bovine Serum (FBS) and 2x concentration of antibiotic-antimycotic (Gibco, Carlsbad, CA) was added to cover the explants. Explants were incubated at 37 °C in a humidified environment of 95% air, 5% CO_2. Three days after plating, the concentration of FBS and antibiotic-antimycotic were reduced to 10% and 1x, respectively. Tracheal segments were removed when the outgrowing cells became locally confluent. Once the 60-mm dish became confluent, cells were harvested by trypsinization and passed to a single 60-mm dish. Tracheal smooth muscle cells were subsequently passaged at a 1:2 ratio. Greater than 90% of these cells from each donor mouse were smooth muscle cells, as determined by immunofluorescence performed by an antibody raised against smooth muscle actin (A2547; Sigma-Aldrich, Saint Louis, MO). All experiments were performed on confluent cells at passage 3.

Ovalbumin immunization

Ovalbumin (100 µg OVA, Sigma-Aldrich, Saint Louis, MO) complexed with aluminum potassium sulfate (1mg, alum) were administered intraperitoneally (i.p.) on

days 1 and 14, and intranasally (i.n.) (50 µg OVA in 50 µL PBS) on days 14, 25, 26, and 27. Control mice received i.p. injections of alum alone and intranasal PBS. Twenty-four hours after the last i.n. dose of OVA (day 28), animals were pre-treated intratracheally with the PI3Kγ MP (15 µg in 50 µL PBS), equimolar amounts of P1 control peptide or vehicle 30 minutes before assessing AHR to inhaled methacholine. To assess the anti-inflammatory action of the PI3Kγ MP, wild-type BALB/c females were treated by intra-tracheal instillation with the PI3Kγ MP (25 µg in a final volume of 50 µL of PBS) or equimolar amounts of P1 control peptide, before each intra-nasal administration of OVA (days 14, 25, 26, and 27).

Airway inflammation analysis

Twenty-four hours after the final OVA injection (day 28), mice were anesthetized (sodium pentobarbital, 70-90 mg/kg, i.p.) and the tracheas incised and cannulated. The airways were washed with 2.5 mL of phosphate-buffered saline solution (PBS) and the total number of cells in the bronchoalveolar lavage (BAL) was determined with a Neubauer hemocytometer. A volume of 50 µL of BAL was centrifuged onto cytospin glass slides at 50 xg at room temperature for 5 minutes and stained with a Diff-Quick system (LabAids, Ronkonkoma, USA). A total of 100 cells per slide were counted and classified as neutrophils, macrophages, lymphocytes and eosinophils on the basis of morphological criteria. Erythrocytes and epithelial cells were ignored and the results were expressed as cells/mL. To assess the peribronchial inflammation, the lungs of a group of animals that had not been subjected to bronchoalveolar lavage were explanted, fixed in a solution of 4% paraformaldehyde (PFA) for 24 hours at 4 °C and embedded in paraffin. 5 µm-thick slices were cut, deparaffinized, stained with a hematoxylin-eosin solution (Bio-Optica, Milano, Italy), dehydrated and mounted with glass coverslips. The extent of peribronchial inflammation was classified as follows: 0- normal; 1- few

inflammatory cells; 3- a thick ring of inflammatory cells. To evaluate the presence of goblet cells, lung slices were stained with periodic acid-Schiff's reagent (PAS) (Bio-Optica, Milano, Italy) and the percentage of PAS-positive cells was calculated by counting the number of PAS-positive epithelial cells and total epithelial cells.

In vivo stability, toxicity and immunogenicity of the PI3Kγ MP

To assess *in vivo* transduction efficiency and stability of the PI3Kγ MP, wild-type BALB/c mice were injected intratracheally with a FITC-conjugated PI3Kγ MP (1.5 µg in a final volume of 50 µL PBS) or vehicle. 30 minutes, 2 hours, 1 day and 4 days after the injection, animals were anesthetized, trachea, lungs and hearts were extracted and frozen in OCT compound. 10 µm cryosections were obtained with a cryostat Leica CM1850 (Leica Microsystems GmbH, Wetzlar, Germany) and bright field and FITC images were acquired with a Zeiss Observer-Z1 microscope, equipped with the Apotome (Carl Zeiss, Oberkochen, Germany).

To evaluate toxicity, mice were injected intratracheally with the PI3Kγ MP (15 µg in a final volume of 50 µL of PBS) or vehicle, daily for 3 weeks. Weight change, lethality and general abnormalities were monitored. To assess liver and kidney toxicity, aspartate aminotransferase, alanine aminotransferase, blood urea nitrogen and creatinine levels in the blood were examined.

To evaluate immunogenicity, antigen-specific IgG were examined by ELISA in the serum of OVA-sensitized mice treated by intra-tracheal instillation with the PI3Kγ MP (25 µg in a final volume of 50 µL of PBS) or equimolar amounts of P1 control peptide, before each intra-nasal administration of OVA (days 14, 25, 26, and 27).

Immunofluorescence staining

HEK 293 cells were fixed for 10 min in 4% paraformaldehyde before permeablization with 0.1% Triton-X. Then cells were blocked by incubation for 1 h at

room temperature with 0.1 ml of phosphate-buffered saline (PBS) containing 5% bovine serum albumin. After blocking, cells were stained by incubation with Phalloidin-561 (1:1000). Image analyses were carried out using Image J software.

Statistical analysis

Prism software (GraphPad Software Inc., La Jolla, CA, USA) was used for statistical analysis. Throughout, all the data were presented as Mean ± SEM and P values were calculated using Student's t-test, one-way and two-way ANOVA followed by Bonferroni's post-hoc comparisons tests, as appropriate.

Figure

Fig. 1

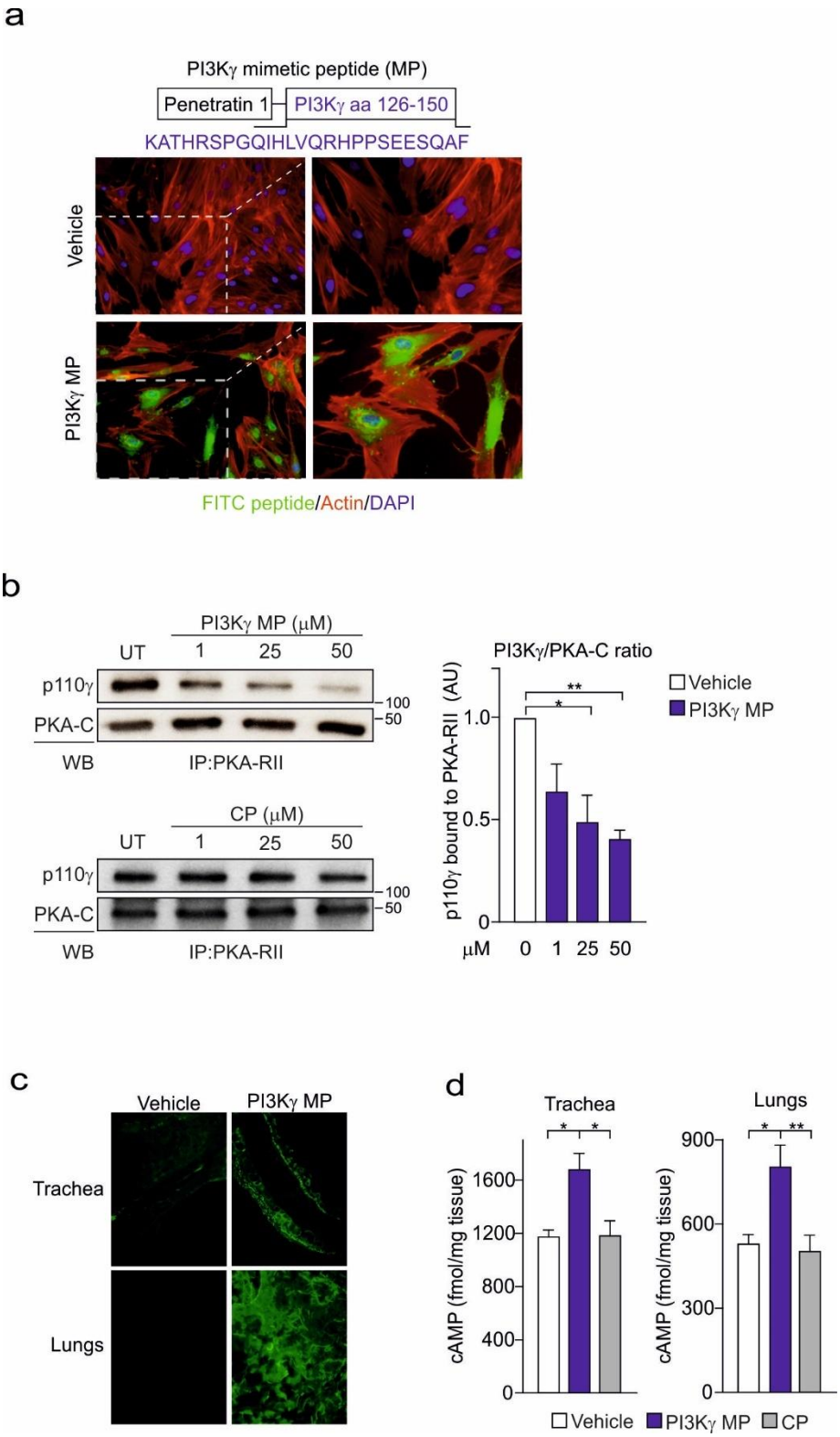
a
PI3Kγ mimetic peptide (MP)
Penetratin 1
PI3Kγ aa 126-150
KATHRSPGQIHLVQRHPPSEESQAF
Vehicle
PI3Kγ MP
FITC peptide/Actin/DAPI
b
PI3Kγ MP (μM)
UT
1
25
50
p110γ
PKA-C
100
50
WB
IP:PKA-RII
CP (μM)
PI3Kγ/PKA-C ratio
p110γ bound to PKA-RII (AU)
Vehicle
PI3Kγ MP
μM
0
1
25
50
c
Vehicle
PI3Kγ MP
Trachea
Lungs
d
Trachea
Lungs
cAMP (fmol/mg tissue)
Vehicle
PI3Kγ MP
CP

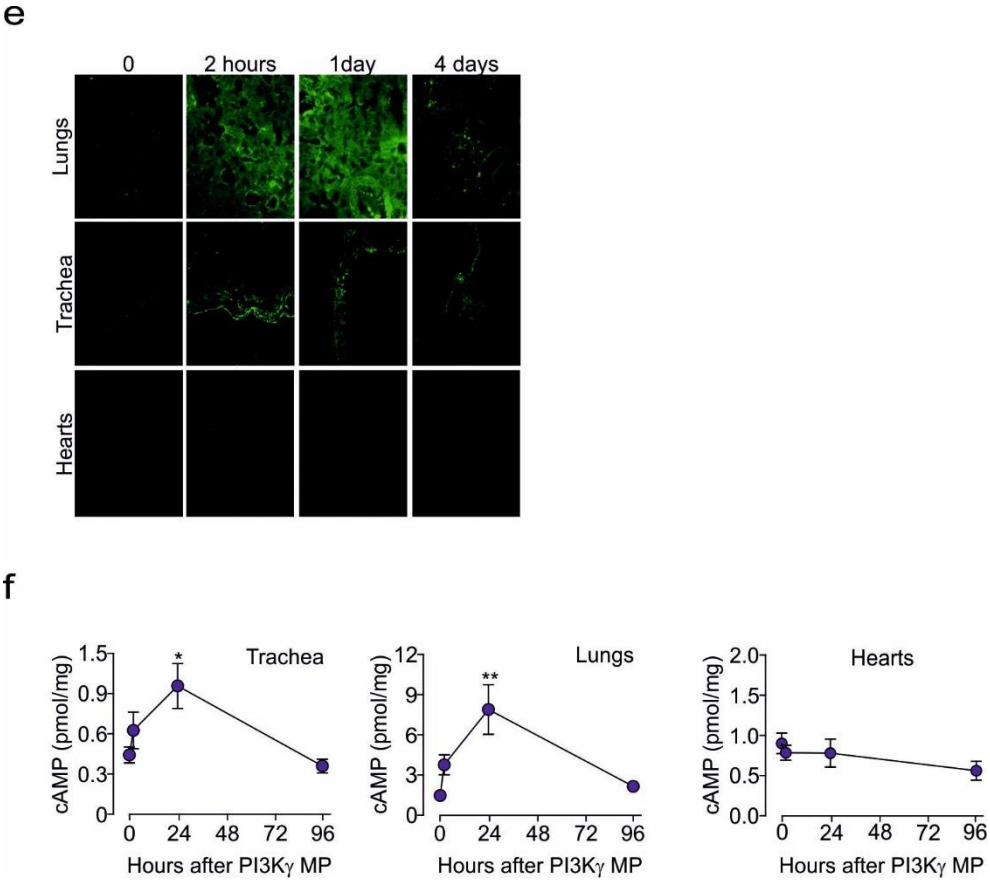

Figure 1. A PI3Kγ mimetic peptide enhances cAMP levels *in vitro* and *in vivo* in the airways by disrupting PI3Kγ/PKA interaction.

(a) Top, schematic representation of the cell-permeable PI3Kγ mimetic peptide (MP). The 126-150 region of PI3Kγ was fused to Penetratin 1 (P1). Bottom, intracellular fluorescence of human bronchial smooth muscle cells (hBSMCs) following one-hour incubation with a FITC-labeled version of the PI3Kγ MP (50 µM) or vehicle. (**b**) Representative immunoblot (left) and relative quantification (right) of the PI3Kγ/PKA-RII complex in HEK 293 cells expressing PI3Kγ and exposed to different doses of the PI3Kγ MP for 2 hours (n = 3). (**c**) Tissue distribution of a FITC-labeled PI3Kγ MP at 30 min after intra-tracheal instillation in BALB/c mice (1.5 µg). (**d**) cAMP levels in tissues from mice treated as in (**c**) (n = 5). (**e**) Tissue distribution of a FITC-labeled PI3Kγ MP at indicated time points after intra-tracheal instillation (1.5 µg) in BALB/c

mice. (**f**) cAMP levels in tissues from mice treated as in (**e**) (n = 5). *P<0.05 and **P<0.01 by one-way ANOVA followed by Bonferroni's post-hoc test. Throughout, data are mean ± SEM.

Fig. 2

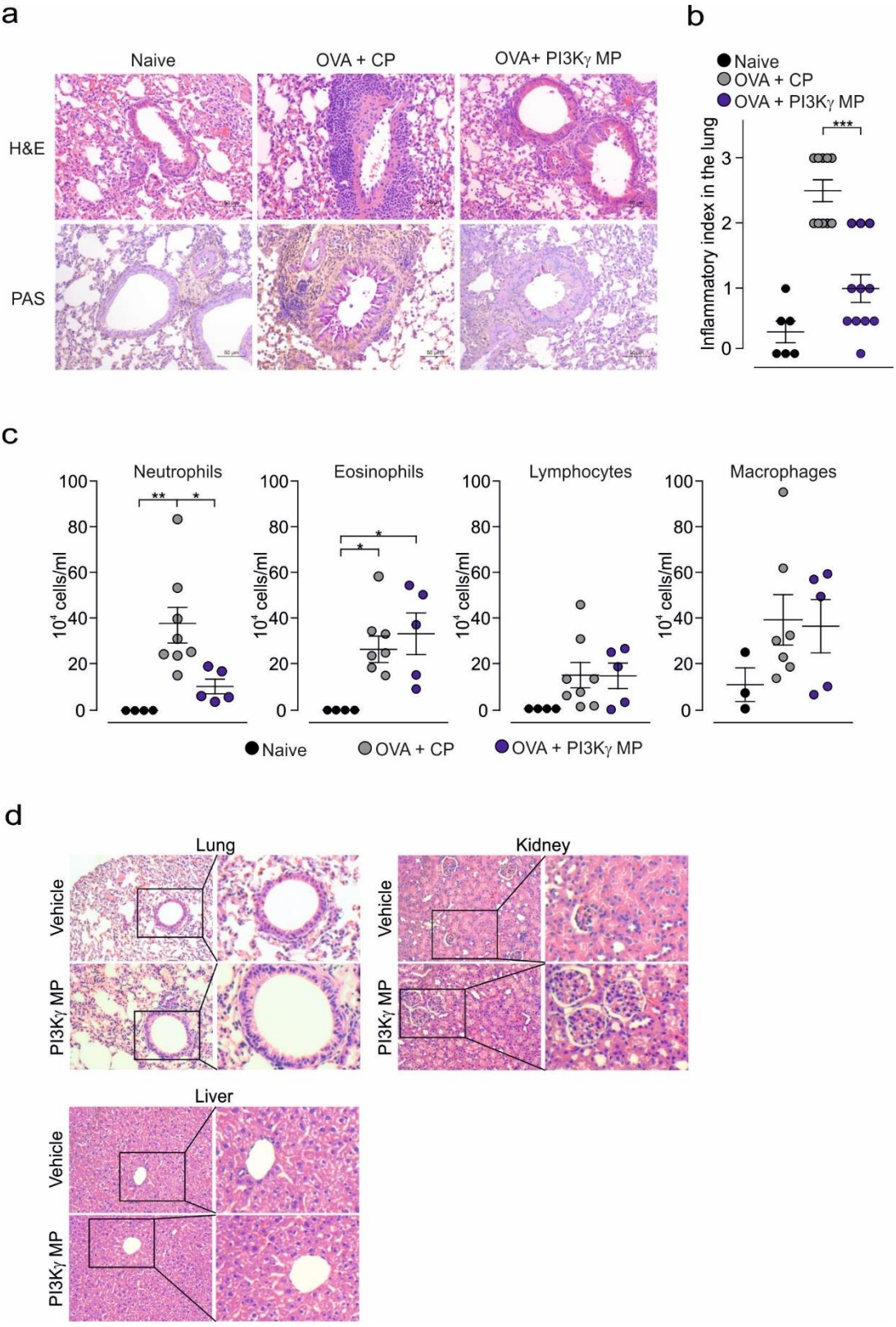
a
Naive
OVA + CP
OVA+ PI3Kγ MP
H&E
PAS
b
Naive
OVA + CP
OVA + PI3Kγ MP
***
Inflammatory index in the lung
0
1
2
3
c
Neutrophils
Eosinophils
Lymphocytes
Macrophages
10⁴ cells/ml
0
20
40
60
80
100
**
*
*
*
Naive
OVA + CP
OVA + PI3Kγ MP
d
Lung
Kidney
Liver
Vehicle
PI3Kγ MP

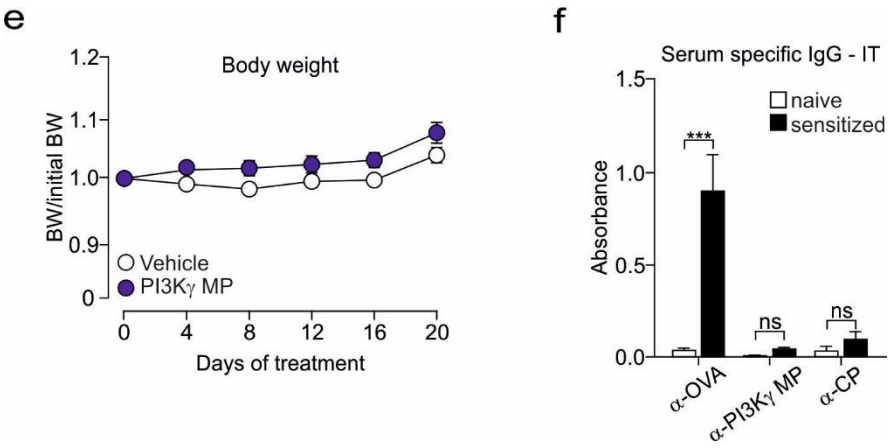

Figure 2. The PI3Kγ MP limits neutrophilic lung inflammation in asthmatic mice. (**a**) Representative images of H&E (top) and periodic acid-Schiff's reagent (bottom) staining of lung sections of naïve and OVA-sensitized mice, pre-treated with PI3Kγ MP (25 µg) or CP (equimolar amount), before each intranasal OVA administration (days 14, 25, 26 and 27 of OVA sensitization protocol). (**b**) Semi-quantitative analysis of peribronchial inflammation in lung sections as shown in (**a**). Naïve, n = 6; OVA + PI3Kγ MP, n = 11; OVA + CP, n = 10. (**c**) Number of neutrophils, macrophages, lymphocytes and eosinophils in the bronchoalveolar lavage (BAL) of mice treated as in (**a**). Naïve, n = 4; OVA + PI3Kγ MP, n = 5; OVA + CP, n = 8. (**d**) Representative H&E staining images of BALB/c mice treated intratracheally with vehicle or 15 µg PI3Kγ peptide daily for 3 weeks. (**e**) Body weight change in BALB/c mice treated as in (**d**). (**f**) Levels of serum specific IgG against OVA, PI3Kγ MP and the control P1 peptide in naïve or OVA-sensitized mice treated as in (**a**) (n = 4). In panels (**b**), (**c**) and (**f**) *P <0.05, **P <0.01 and ***P <0.001 by one-way ANOVA followed by Bonferroni's post-hoc test. Throughout, data are mean ± SEM. *P<0.05 and ***P<0.01 by one-way ANOVA followed by Bonferroni's post-hoc test. Data are the mean ± SEM.

Fig. 3

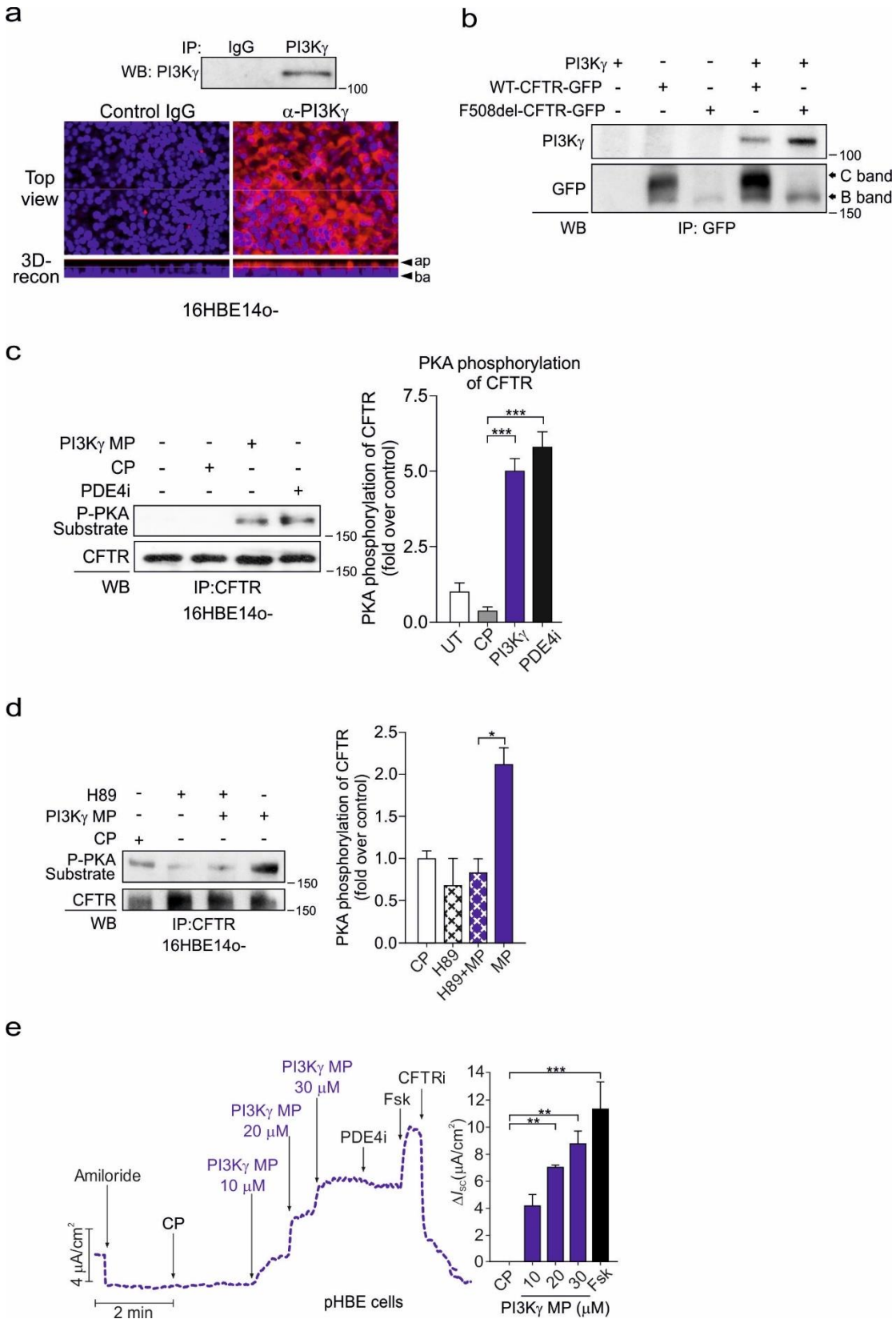
a
IP: IgG PI3Kγ
WB: PI3Kγ
100
Control IgG
α-PI3Kγ
Top view
3D-recon
ap
ba
16HBE14o-
b
PI3Kγ + - - + +
WT-CFTR-GFP - + - + -
F508del-CFTR-GFP - - + - +
PI3Kγ
GFP
100
C band
B band
150
WB
IP: GFP
c
PI3Kγ MP - - + -
CP - + - -
PDE4i - - - +
P-PKA Substrate
CFTR
150
150
WB
IP:CFTR
16HBE14o-
PKA phosphorylation of CFTR
PKA phosphorylation of CFTR (fold over control)
7.5
5.0
2.5
0.0
***
***
UT
CP
PI3Kγ
PDE4i
d
H89 - + + -
PI3Kγ MP - - + +
CP + - - -
P-PKA Substrate
CFTR
150
150
WB
IP:CFTR
16HBE14o-
PKA phosphorylation of CFTR (fold over control)
2.5
2.0
1.5
1.0
0.5
0.0
*
CP
H89
H89+MP
MP
e
Amiloride
CP
PI3Kγ MP 10 μM
PI3Kγ MP 20 μM
PI3Kγ MP 30 μM
PDE4i
Fsk
CFTRi
4 μA/cm²
2 min
pHBE cells
ΔIsc(μA/cm²)
14
12
10
8
6
4
2
0
***
**
**
CP
10
20
30
Fsk
PI3Kγ MP (μM)

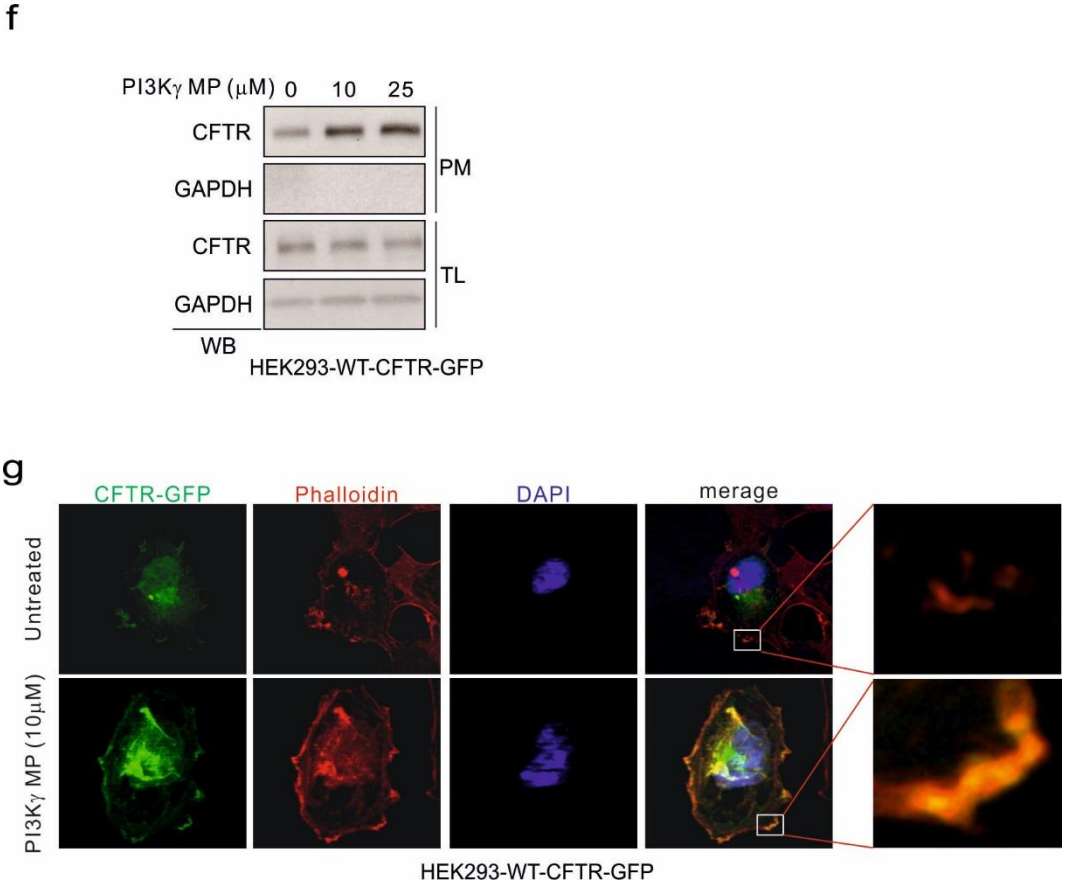

Figure 3. The PI3Kγ MP is a wild-type CFTR potentiator.

(a) Top, immunoblot of PI3Kγ immunoprecipitation (IP) in human normal bronchial epithelial cells (16HBE14o-). Normal mouse IgG was used for control IP. Bottom, confocal images of PI3Kγ localization in 16HBE14o- cells. x-y images from just below the apical membrane and x-z images generated by 3D reconstruction are shown. ap: apical and ba: basal. (**b**) Co-immunoprecipitation of PI3Kγ with wild-type and F508del CFTR in HEK 293 cells expressing PI3Kγ together with either WT-CFTR-GFP or F508del-CFTR-GFP. (**c**) Representative Western Blot (left) and relative quantification (right) of PKA-mediated phosphorylation of CFTR in 16HBE14o- cells treated with vehicle, CP (25 μM), PI3Kγ MP (25 μM) and the PDE4 inhibitor Rolipram (PDE4i; 10 μM) for 30 min (n = 4). (**d**) Representative Western Blot (left) and relative quantification (right) of PKA-mediated phosphorylation of CFTR in 16HBE14o- cells

treated with CP (25 μM), the PKA inhibitor H89 (5 μM), PI3Kγ MP (25 μM) together with H89 and PI3Kγ MP (25 μM). (**e**) Representative trace of I_{SC} measured in Ussing chambers (left) and average current variations in response to the indicated treatments (right) in primary human normal bronchial epithelial (pHBE) cells (n = 3). The following treatments were applied at the indicated times: ENaC inhibitor amiloride (10 μM), CP (30 μM), PI3Kγ MP (10-30 μM), PDE4 inhibitor Rolipram (PDE4i; 10 μM), forskolin (Fsk, 10 μM) and CFTR inhibitor 172 (CFTRi; 20 μM). (**f**) Western blot detection of surface WT CFTR in HEK 293 cells, that were exposed to the PI3Kγ MP at indicated concentration (0, 10, 25 μM) and subjected to cell surface biotinylation assay. PM, plasma membrane; TL, total lysate. (**g**) representative images of surface WT CFTR co-localization with actin. Top, HEK 293 cells were transfected with WT-CFTR overnight. Bottom, HEK 293 cells were transfected with WT-CFTR overnight then treated with PI3Kγ MP (10 μM) 2 h. Throughout, *P <0.05, **P <0.01 and ***P <0.001 by one-way ANOVA followed by Bonferroni's post-hoc test; data are mean ± SEM. In panels (**b**), (**c**) and (**d**), representative Western blot images of 3 independent experiments are shown.

Fig. 4

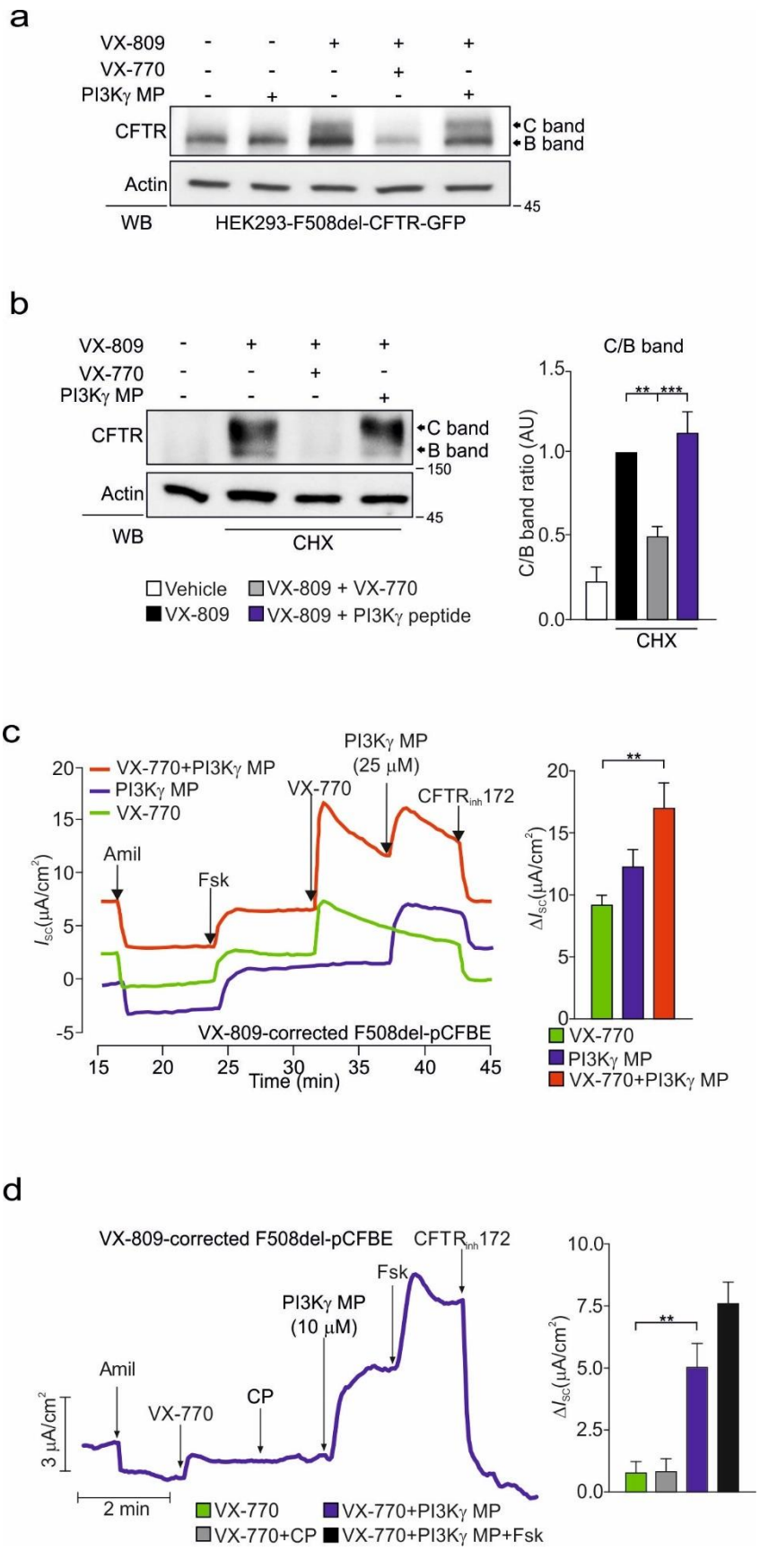
a
VX-809
VX-770
PI3Kγ MP
CFTR
C band
B band
Actin
45
WB
HEK293-F508del-CFTR-GFP
b
VX-809
VX-770
PI3Kγ MP
CFTR
C band
B band
150
Actin
45
WB
CHX
Vehicle
VX-809
VX-809 + VX-770
VX-809 + PI3Kγ peptide
C/B band
C/B band ratio (AU)
1.5
1.0
0.5
0.0
**
***
CHX
c
VX-770+PI3Kγ MP
PI3Kγ MP
VX-770
PI3Kγ MP
(25 μM)
VX-770
CFTRinh172
Amil
Fsk
Isc(μA/cm2)
20
15
10
5
0
-5
VX-809-corrected F508del-pCFBE
15
20
25
30
35
40
45
Time (min)
**
ΔIsc(μA/cm2)
VX-770
PI3Kγ MP
VX-770+PI3Kγ MP
d
VX-809-corrected F508del-pCFBE
CFTRinh172
Fsk
PI3Kγ MP
(10 μM)
Amil
VX-770
CP
3 μA/cm2
2 min
VX-770
VX-770+PI3Kγ MP
VX-770+CP
VX-770+PI3Kγ MP+Fsk
ΔIsc(μA/cm2)
10.0
7.5
5.0
2.5
0.0
**

Figure 4. The PI3Kγ MP enhances the stabilization and chloride conductance function of rescued F508del CFTR.

(a) Western blot detection of CFTR in HEK 293 cell expressing F508del-CFTR, cells were treated with PI3Kγ MP (25 μM), VX-770 and VX-809 (5 μM) for 48 h as indicated. **(b**) Western blot detection of CFTR in HEK 293 cell expressing F508del-CFTR, cells were treated as in (**a**) followed by 6 h CHX (100 μg/ mL) treatment. **(c**) Left, Representative trace of I_{SC} measured in Ussing chambers in primary human CF bronchial epithelial cells (F508del/F508del) corrected with VX-809 (5 μM) for 48 hours and then exposed to the following drugs at the indicated times: Amiloride (Amil, 10 μM), forskolin (Fsk, 10 μM), VX-770 (10 μM), PI3Kγ MP (PI3Kγ, 25 μM), and CFTR inhibitor 172 ($CFTR_{inh}$ 172; 20 μM). Right, Average total current variation in response to /treatment with Fsk plus: VX-770, PI3Kγ MP or both (VX-770 + PI3Kγ MP) (n=4). (**d**) Left, Representative trace of I_{SC} measured in Ussing chambers in primary human CF bronchial epithelial cells (F508del/F508del) corrected with VX-809 (5 μM, 48 hours) and then exposed sequentially to Amil (10 μM), VX-770 (10 μM), CP (10 μM), PI3Kγ MP (10 μM), Fsk (10 μM) and $CFTR_{inh}$ 172 (20 μM). Right, Average current variations in response to the indicated treatments (n=3). Throughout, **P <0.01 and ***P <0.001 by one-way ANOVA followed by Bonferroni's post-hoc test; data are mean ± SEM. In panels (**a**) and (**b**), representative Western blot images of 3 independent experiments are shown.

Fig. 5

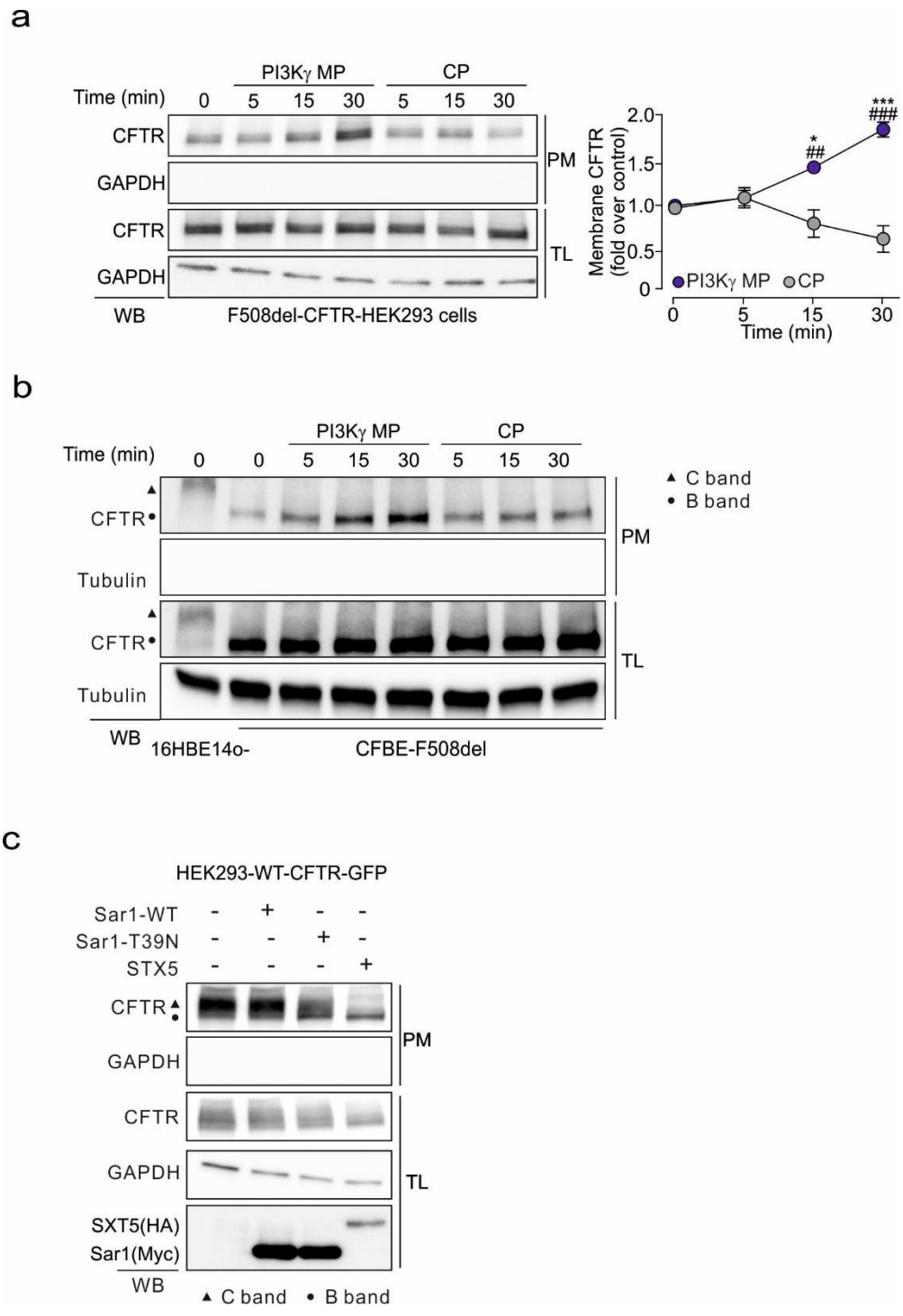
a
PI3Kγ MP
CP
Time (min)
0
5
15
30
5
15
30
CFTR
GAPDH
CFTR
GAPDH
PM
TL
WB
F508del-CFTR-HEK293 cells
Membrane CFTR (fold over control)
2.0
1.5
1.0
0.5
0
*
##
***
###
PI3Kγ MP
CP
0
5
15
30
Time (min)
b
PI3Kγ MP
CP
Time (min)
0
0
5
15
30
5
15
30
C band
B band
CFTR
Tubulin
CFTR
Tubulin
PM
TL
WB
16HBE14o-
CFBE-F508del
c
HEK293-WT-CFTR-GFP
Sar1-WT
Sar1-T39N
STX5
CFTR
GAPDH
CFTR
GAPDH
SXT5(HA)
Sar1(Myc)
PM
TL
WB
C band
B band

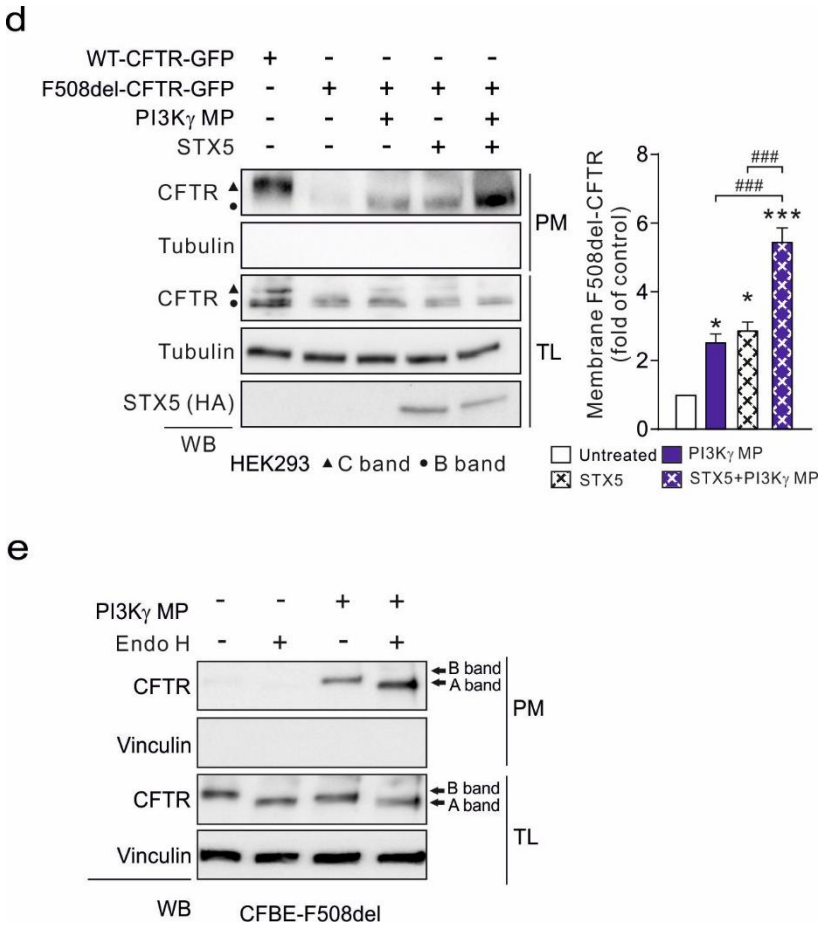

Figure 5. The PI3Kγ MP enhances the surface expression of F508del CFTR via an unconventional pathway.

(**a**) Left, representative Western blot detection of surface CFTR in HEK 293 cells transfected with F508del CFTR overnight, followed by treatment with the PI3Kγ MP (10 μM) at indicated time (5, 15, 30 min) before cell surface biotinylation assay. PM, plasma membrane; TL, total lysate. Right, relative quantification of CFTR at the plasma membrane. (**b**) Western blot detection of surface CFTR in CFBE-F508del cells, that were exposed to the PI3Kγ MP at indicated times (0, 5, 15, 30 minutes) and subjected to cell surface biotinylation assay. (**c**) surface CFTRs were detected in HEK 293 cells co-transfection with WT-CFTR and Sar1-WT, Sat1-T39N or STX5 overnight. (**d**) Left, representative Western blot detection of surface CFTR in HEK 293 cells that were

transfected with F508del-CFTR or co-transfected with F508del-CFTR and STX5 overnight, then 15 min after exposure to PI3Kγ MP (10 μM) cells were subjected to surface biotinylation assay. Right, relative quantification of CFTR at the plasma membrane. (**e**) Surface biotinylated F508del-CFTRs were treated with endoglycosidase H (Endo H) that deglycosylates ER core-glycosylation but not complex-glycosylation, and forms a band shift (from B to A). In panels (**a**), *P<0.05 and ****P*<0.001 versus un-treatment control and ### *P*<0.001 versus CP by two-way ANOVA followed by Bonferroni's post-hoc test. In panels (**d**), *P<0.05, **P<0.01 and ****P*<0.001 versus un-treatment control and ### *P*<0.001 by two-way ANOVA followed by Bonferroni's post-hoc test. Throughout, data are mean ± SEM. All the experiments were repeated at least 3 independent times.

Tables

Table I

Blood biochemical test in mice treated with vehicle or PI3Kγ MP

	ALT (U/L)	AST (U/L)	Urea (mg/dl)	Creatinine (mg/dl)
Vehicle	35.00 ± 4.472	136.7 ± 36.21	63.67±2.33	0.16±0.03
PI3Kγ MP	37.00 ± 10.44^{ns}	145.7 ± 12.12^{ns}	68±3.51 ^{ns}	0.18±0.03 ^{ns}

Legend:

ALT: Alanine aminotransferase Normal clinical value in mice: 17-77 U/L.

AST: Aspartate aminotransferase. Normal clinical value in mice: 54-298 U/L.

Creatinine: Normal clinical value in mice: 0.3-1.0mg/dl

ns: not significant.

Table II

Echocardiographic analysis of mice treated with vehicle or PI3Kγ MP

	PI3Kγ MP (n=7)	Vehicle(n=7)	P
LVEF (%)	56.75±4.46	60.49±2.23	n.s
FS (%)	36.74±4.59	32.05±1.51	n.s
IVSd (mm)	0.50±0.04	0.61±0.04	n.s
IVSs (mm)	0.93±0.04	1.04 ±0.05	n.s
LVIDd (mm)	3.99 ±0.05	4.11 ±0.09	n.s
LVIDs (mm)	2.71±0.06	2.80 ±0.11	n.s
LVPWd (mm)	0.52 ±0.03	0.56±0.02	n.s
LVPWs (mm)	0.85 ±0.04	0.88 ±0.03	n.s
LVM/BW	2.7±0.22	2.97±0.25	n.s

[a] **Abbreviations: LVEF, left ventricular ejection fraction; FS, fractional shortening; LVSd, interventricular septum end-diastole; LVSs, interventricular septum end-systole; LVIDd, left ventricular internal diameter end-diastole; LVIDs, left ventricular internal diameter end-systole; LVPWd, left ventricular posterior wall end-diastole; LVPWs, left ventricular posterior wall end-systole; LVM/BW, left ventricular mass / body weight (mg/g).**

[b] Data are presented as Mean ± SEM.

Bibliography

[1] P. Calverley and P. Walker, “Chronic obstructive pulmonary disease,” *Lancet*, vol. 362, no. 9389, pp. 1053–1061, Sep. 2003.

[2] “WHO (2017) Chronic obstructive pulmonary disease (COPD). WHO, Geneva, Switzerland.”

[3] S. I. Rennard and M. B. Drummond, “Early chronic obstructive pulmonary disease: definition, assessment, and prevention,” *Lancet*, vol. 385, no. 9979, pp. 1778–1788, May 2015.

[4] F. Nurwidya, T. Damayanti, and F. Yunus, “The Role of Innate and Adaptive Immune Cells in the Immunopathogenesis of Chronic Obstructive Pulmonary Disease.,” *Tuberc. Respir. Dis. (Seoul).*, vol. 79, no. 1, pp. 5–13, Jan. 2016.

[5] P. J. Barnes, “Glucocorticosteroids: current and future directions.,” *Br. J. Pharmacol.*, vol. 163, no. 1, pp. 29–43, May 2011.

[6] P. J. Barnes, “Distribution of Receptor Targets in the Lung,” *Proc. Am. Thorac. Soc.*, vol. 1, no. 4, pp. 345–351, Dec. 2004.

[7] B. Beghè, K. F. Rabe, and L. M. Fabbri, “Phosphodiesterase-4 Inhibitor Therapy for Lung Diseases,” *Am. J. Respir. Crit. Care Med.*, vol. 188, no. 3, pp. 271–278, Aug. 2013.

[8] R. C. Boucher, “New concepts of the pathogenesis of cystic fibrosis lung disease.,” *Eur. Respir. J.*, vol. 23, no. 1, pp. 146–58, Jan. 2004.

[9] S. V. Raju, G. M. Solomon, M. T. Dransfield, and S. M. Rowe, “Acquired Cystic Fibrosis Transmembrane Conductance Regulator Dysfunction in Chronic Bronchitis and Other Diseases of Mucus Clearance.,” *Clin. Chest Med.*, vol. 37, no. 1, pp. 147–58, Mar. 2016.

[10] C. E. Wainwright *et al.*, “Lumacaftor–Ivacaftor in Patients with Cystic Fibrosis Homozygous for Phe508del *CFTR*,” *N. Engl. J. Med.*, vol. 373, no. 3, pp. 220–231, Jul. 2015.

[11] A. Perino *et al.*, “Integrating Cardiac PIP3 and cAMP Signaling through a PKA Anchoring Function of p110??,” *Mol. Cell*, vol. 42, no. 1, pp. 84–95, 2011.

[12] A. Ghigo *et al.*, “Phosphoinositide 3-Kinase Protects Against Catecholamine-Induced Ventricular Arrhythmia Through Protein Kinase A-Mediated Regulation of Distinct Phosphodiesterases,” *Circulation*, vol. 126, no. 17, pp. 2073–2083, Oct. 2012.

[13] G. M. Denning, M. P. Anderson, J. F. Amara, J. Marshall, A. E. Smith, and M. J. Welsh, “Processing of mutant cystic fibrosis transmembrane conductance

regulator is temperature-sensitive," *Nature*, vol. 358, no. 6389, pp. 761–764, Aug. 1992.

[14] C. M. F. Miguel J Lobo, Margarida D Amaral, Manuela Zaccolo, "EPAC1 activation by cAMP stabilizes CFTR at the membrane by promoting its interaction with NHERF1," no. May, 2016.

[15] P. M. QUINTON, "Physiological Basis of Cystic Fibrosis: A Historical Perspective," *Physiol. Rev.*, vol. 79, no. 1, pp. S3–S22, Jan. 1999.

[16] C. L. Ward, S. Omura, and R. R. Kopito, "Degradation of CFTR by the ubiquitin-proteasome pathway.," *Cell*, vol. 83, no. 1, pp. 121–7, Oct. 1995.

[17] M. D. Amaral, "CFTR and Chaperones: Processing and Degradation," *J. Mol. Neurosci.*, vol. 23, no. 1–2, pp. 041–048, 2004.

[18] H. Y. Gee, S. H. Noh, B. L. Tang, K. H. Kim, and M. G. Lee, "Rescue of ΔF508-CFTR Trafficking via a GRASP-Dependent Unconventional Secretion Pathway," *Cell*, vol. 146, no. 5, pp. 746–760, 2011.

[19] M. ZORKO and U. LANGEL, "Cell-penetrating peptides: mechanism and kinetics of cargo delivery," *Adv. Drug Deliv. Rev.*, vol. 57, no. 4, pp. 529–545, Feb. 2005.

[20] V. K. Raker, C. Becker, and K. Steinbrink, "The cAMP Pathway as Therapeutic Target in Autoimmune and Inflammatory Diseases.," *Front. Immunol.*, vol. 7, p. 123, 2016.

[21] V. Saint-Criq and M. A. Gray, "Role of CFTR in epithelial physiology.," *Cell. Mol. Life Sci.*, vol. 74, no. 1, pp. 93–115, 2017.

[22] D. C. GADSBY and A. C. NAIRN, "Control of CFTR Channel Gating by Phosphorylation and Nucleotide Hydrolysis," *Physiol. Rev.*, vol. 79, no. 1, pp. S77–S107, Jan. 1999.

[23] M. J. Watson *et al.*, "The Cystic Fibrosis Transmembrane Conductance Regulator (CFTR) Uses its C-Terminus to Regulate the A2B Adenosine Receptor," *Nat. Publ. Gr.*, 2016.

[24] G. Veit *et al.*, "Some gating potentiators, including VX-770, diminish F508-CFTR functional expression," *Sci. Transl. Med.*, vol. 6, no. 246, p. 246ra97-246ra97, Jul. 2014.

[25] D. M. Cholon *et al.*, "Potentiator ivacaftor abrogates pharmacological correction of F508 CFTR in cystic fibrosis," *Sci. Transl. Med.*, vol. 6, no. 246, p. 246ra96-246ra96, Jul. 2014.

[26] K. M. Cihil, P. Ellinger, A. Fellows, D. B. Stolz, D. R. Madden, and A. Swiatecka-Urban, "Disabled-2 Protein Facilitates Assembly Polypeptide-2-independent

Recruitment of Cystic Fibrosis Transmembrane Conductance Regulator to Endocytic Vesicles in Polarized Human Airway Epithelial Cells," *J. Biol. Chem.*, vol. 287, no. 18, pp. 15087–15099, Apr. 2012.

[27] M. D. Amaral and C. M. Farinha, "Rescuing mutant CFTR: a multi-task approach to a better outcome in treating cystic fibrosis.," *Curr. Pharm. Des.*, vol. 19, no. 19, pp. 3497–508, 2013.

[28] C. Rabouille, "Pathways of Unconventional Protein Secretion," 2017.

[29] W. Hong, "SNAREs and traffic," *Biochim. Biophys. Acta - Mol. Cell Res.*, vol. 1744, no. 2, pp. 120–144, Jun. 2005.

[30] J.-S. Yoo, B. D. Moyer, S. Bannykh, H.-M. Yoo, J. R. Riordan, and W. E. Balch, "Non-conventional Trafficking of the Cystic Fibrosis Transmembrane Conductance Regulator through the Early Secretory Pathway," *J. Biol. Chem.*, vol. 277, no. 13, pp. 11401–11409, Mar. 2002.

[31] H. Y. Gee, B. L. Tang, K. H. Kim, and M. G. Lee, "Syntaxin 16 binds to cystic fibrosis transmembrane conductance regulator and regulates its membrane trafficking in epithelial cells.," *J. Biol. Chem.*, vol. 285, no. 46, pp. 35519–27, Nov. 2010.

[32] G. Barisione, M. Baroffio, E. Crimi, and V. Brusasco, "Beta-Adrenergic Agonists.," *Pharmaceuticals (Basel).*, vol. 3, no. 4, pp. 1016–1044, Mar. 2010.

[33] W. M. Brown, "Treating COPD with PDE 4 inhibitors.," *Int. J. Chron. Obstruct. Pulmon. Dis.*, vol. 2, no. 4, pp. 517–33, 2007.

[34] K. Fosgerau and T. Hoffmann, "Peptide therapeutics: current status and future directions," *Drug Discov. Today*, vol. 20, no. 1, pp. 122–128, Jan. 2015.

[35] J. L. Lau and M. K. Dunn, "Therapeutic peptides: Historical perspectives, current development trends, and future directions," *Bioorg. Med. Chem.*, vol. 26, no. 10, pp. 2700–2707, Jun. 2018.

[36] D. W. McGraw *et al.*, "Transgenic overexpression of beta(2)-adrenergic receptors in airway smooth muscle alters myocyte function and ablates bronchial hyperreactivity.," *J. Biol. Chem.*, vol. 274, no. 45, pp. 32241–7, Nov. 1999.

Acknowledgments

I would like to thank all the people who have helped me in my 4-year Ph.D study. Without your support and advice, my work and this thesis could not be completed.

I owe my sincere gratitude to my primary supervisor, Prof. Emilio Hirsch, for his consistent support and encouragement. My deepest gratitude is given to my co-supervisors, Prof. Alessandra Ghigo, especially for her guidance in scientific thinking and solving problems during the past four years.

I am very indebted to everyone in Molecular Biotechnology Center. I would also like to express my gratitude to Alessandra Murabito and Flora Pirozzi who contribute many important data to this project, as well as to Prof. Roberto Lima and MingChuan Li who help and encourage me at any time. It is a great time being with Valentina Sala, Paolo Ettore Porporato, Jean Piero Margaria, Federico Gulluni, Maria Chiara De Santis, Carlo Cosimo Campa, Miriam Matina, Myriam Hsu, Abhishek Derle, Edoardo Ratto, Wyart Elisabeth, Luca Rossi and Luca Gozzelino in the lab.

I would like to thank my parents, my daughters and my wife especially for their love, understanding encouragement and support during my study.

I am grateful to Prof. Fan Cheng and Prof. Xiaoyun Lu who provided much support to me when I applied for the Ph.D fellowship and during my 4-years study. I would also say thanks to Ligang Ren.....